

4 Photon spectrometers

At the time before the invention of radiation detectors with help of which one can discriminate between different radiation energies, a separation of the components to be determined from the sample matrix was necessary during activation analysis - preferably carried out after activation, since inactive contamination after radiation exposure does no harm to the analysis. The activities of the resulting different fractions were then measured separately. Gas ionisation detectors e.g. Geiger-Müller counting tubes were used for activity counting. In the case of beryllium or deuterium analysis by photodisintegration, neutron counting tubes or secondary targets (photoneutron activation foils) had to be used as noted above. After the advent and general availability of photon spectrometers almost invariably these devices have been utilised for activation analysis since most of the product nuclides of any nuclear activation process emit typical photon spectra including gamma and specific X-radiation which can easily be discriminated (see chapter 2). Thus, components of an irradiated sample can be analysed without a chemical separation before or after activation. Moreover, with help of advanced spectrometry technology simultaneous analyses of several radionuclides (multi-component analyses) have become possible. Product nuclide radiation other than photons have been used in exceptional cases only, e.g. if the product nuclide does not emit specific photon energies. However, in these cases instead of undertaking tedious separation procedures one would generally apply another activation method producing gamma-ray emitting radionuclides or another analysis method. Another advantage of photon counting is that absorption of the radiation within the sample matrix mostly is negligible whereas in the case of beta or, even worse, alpha particle counting it might lead to severe misinterpretations of the spectra and miscalculation during quantitative data evaluation. Only in the case of very soft X-radiation used for analysis one has to be aware of significant self-absorption, as is demonstrated in Ch.6. Due to all the mentioned advantages, photon spectroscopy has become the most frequently applied activity measurement method - not only in activation analysis. In this chapter, the photon spectrometers are discussed in more detail. This is done because the analyst in the activation analysis laboratory (to whom this book is devoted) generally is much more concerned with the spectrometers than with the activating radiation sources. The analyst usually does the entire photon spectrometry work by himself whilst the accelerator is run by another operating staff.

Two basic principles of photon counting have been in use, namely the detection by scintillators exploiting the radioluminescence effect and the detection by semiconductor crystals. By both detector types, photons are converted into electric pulses whose heights are quasi-linearly dependent upon the energies of the absorbed photon quanta - at least in the energy region of interest in photon activation analysis (5-3000 keV; see chapters 2 and 5). The pulses are then amplified, reshaped and finally discriminated by their heights with the help of electronic devices which are discussed separately in the following paragraphs. The resulting spectra are then processed by computer.

To shortly summarise all parts of a photon spectrometer necessary for activation analysis³³¹:

- 1 - Detector; scintillation crystal plus photomultiplier or semiconductor crystal and operating voltage supply
- 2 - Preamplifier, voltage or charge-sensitive, plus power supply
- 3 - Linear spectroscopy amplifier; including pile-up rejector and pulse shaping unit
- 4 - Pulse height analyser plus data storage and data output unit which is coupled to a data dumping unit or processing device, e.g. computer

There are various additional optional units for special procedure requirements, of course, but the minimum instrumentation needed consists of the above listed ones.

In the following, the fundamental functional principles of the detectors and electronic analysis systems will not be discussed in detail. Major attention is paid to the analytically relevant properties of the spectrometers in order to provide an aid for the analyst to select the proper system suitable for the given task. Also the required computer software for spectral data evaluation will be discussed only briefly. Since the required instrumentation for radiation spectrometry and data processing is exactly the same as used in "classical" neutron activation - with a few exceptions - excellent fundamental descriptions and discussions can be found in a large number of earlier works. This also applies to the the historical development of the photon spectrometers. Hence, in the following paragraphs, only a short summary of their history is given.

Also, the fabrication of the different kinds of detectors is not discussed; the reader can find information about this problem in Ref's. 332-339. See also Ref's. 678-680.

4.1 Detectors

At this stage it is of use to briefly summarise the different kinds of interaction of photons with matter, especially with material used for the detection of photons. Three relevant processes for photon detection can be distinguished, namely a) the photoelectric effect, b) the Compton scattering, c) the pair production. The probability of their occurrence within a given element is contingent upon the energy of the incident photon. Among these, the photoelectric effect is of major analytical interest whilst all others, if occurring, have to be considered as sources of interference during analysis.

a) In the photoelectric process all of the energy of the incident photon is absorbed by a bound electron of a target atom reappearing as kinetic energy of this electron as it is ejected from the atom. The energy of the ejected electron will then equal the difference between the energy of the incident photon and the binding energy of the level from which the electron was ejected. Although some energy is absorbed by recoil of the target atom nucleus, this is negligible compared with the energy of the incident gamma-ray and the photoelectron. If the incident photon energy exceeds the K-shell binding level, interaction will take place principally with electrons of this shell. As a result of this process the atom is left with a vacancy in this shell, resulting in the emission of specific X-ray quanta or Auger electrons. In the low photon energy region the photoelectric effect dominates, (see paragraphs 4.1.1 and 4.1.2). It is probable that a fraction of the mentioned X-rays escape from the detector. In this case signals will be detected which are representative for the full incident photon energy minus the emitted X-ray energy. The important characteristic of the photoelectric effect is that monoenergetic photons which interact by the photo process will produce monoenergetic photoelectrons within the detector volume which results, through different subsequent processes within the detector, in a uniform, discrete signal which then can be processed.

b) In the Compton scattering process incident photons are scattered by target atom electrons accompanied by a partial energy loss. In this process, scattering generally occurs with electrons which can be regarded as essentially free, and the energy of the incident photon is distributed between the target electron and the scattered photon. This distribution does not have a fixed value but ranges within a relatively large energy interval, depending upon the incoming photon energy. Thus, the Compton process results in a broad electron energy distribution, and therefore, detector pulses originating from Compton scattering cannot be used for evaluation of photon spectra measured after activation,

but rather are unwanted sources of interference, as noted above. At low initial photon energies, a gamma-ray may be elastically scattered from a bound electron with the atom remaining in its initial state. This process does not yield any energy change, yet it plays an important role in the integral efficiency assessment of a detector. The cross section for this process - called coherent scattering - must not be considered in the discussion of the total absorption cross section since it does not leave any energy in the detector. The relationship between the energies of the incoming and the scattered photon is given by the following expressions:

$$E_{\gamma'} = \frac{E_{\gamma}}{1 + \frac{E_{\gamma}}{m_{0e} \cdot c^2} \cdot (1 - \cos \varphi)}$$

$$E_{e'} = E_{\gamma} - E_{\gamma'}$$

where E_{γ} is the incident photon energy, $E_{\gamma'}$ the scattered photon energy, $E_{e'}$ the scattered electron energy and φ the scattering angle. From these expressions one can deduce that the Compton electron energy spectrum extends from zero energy ($\varphi = 0$) up to a maximum energy ($\varphi = \pi$) which is somewhat less than the incident photon energy. The energy distribution of the scattered photons varies from the initial photon energy down to a minimum value which always is less than $m \cdot c^2/2$ (= 255.5 keV).

c) Pair production; if the incoming photon has an energy which exceeds the electron/positron pair rest mass (= 1022 keV), then a production of this pair becomes possible. This process occurs in the coulomb field in the close neighbourhood of the nucleus. The incident photon ray disappears and the pair is created. Its total energy will equal the energy of the primary photon, and the kinetic energy of both particles will be equal to their total energy minus their rest energy ($2m \cdot c^2 = 1022$ keV). Since the positron is unstable, as it comes to rest in the field of an electron, annihilation of the two particles occurs with the emission of two photons, in energy equal to the rest mass equivalent of the pair ($2 \cdot 511$ keV). Interaction by the pair process in a detector will therefore result in an energy loss equal to the incident photon energy minus 1022 keV, if both 511 keV annihilation quanta escape from the detector. If

only one of them escapes, a signal representative for the total incident photon energy minus 511 keV will appear.

Consequently, all in all, various kinds of interaction of photon rays, in energies exceeding 1022 keV, within a detector body will result in a quite complex pulse amplitude spectrum containing signals representative for any energy from zero up to the full energy of the primary photon. Moreover, it is rendered even more complex by other effects, e.g., due to the close environment of the detector as is explained in the following paragraphs.

Other signals also appear which are not due to the measured sample activity at all; they originate from external radiation penetrating the detector shielding or from radioactive contaminations within the shielding material. These signals are called external background. This background has to be known very well to avoid misinterpretations of pulse height spectra obtained from unknown samples.

4.1.1 Scintillation detectors

The first of all particle detection principles used was scintillation counting. It was introduced in the beginning of this century. Visible light flashes were produced on a zinc sulphide screen by alpha particles. The counting was performed by numbering the flashes during visual inspection. Fundamental work on the theory and practice of inorganic scintillators by Hofstadter and McIntyre (Ref's. ^{340,341}) and by Sciver and Hofstadter³⁴² yielded that thallium-activated sodium iodide single crystals were the most suitable scintillators for gamma detection. See also Ref's. ^{343-364,895}.

Organic including liquid scintillators are not discussed in this book since they are not used for photon spectroscopy. An excellent review on the development of sodium iodide detectors and photomultipliers is given by Adams and Dams³⁶⁵.

Thallium activation influences the fluorescence behaviour of the NaI-crystal; this problem is not discussed further. The reader might refer to Ref's. ^{354,366-378,516} for more information.

A schematic representation of a scintillation detector is given in Fig.4.1. Light flashes are produced via secondary electrons from photoelectric effect, Compton scattering or interactions due to pair production if X-rays or gamma photons are absorbed within the crystal (see above). These flashes produce

produce photoelectrons in a photocathode. The electrons are directed to a photomultiplier which is connected to an operating voltage of usually about 1 kV. By secondary electron emission, the incident electron pulses whose heights show a linear dependency upon the energy of the incoming photons are amplified and then can be processed in the following electronic system of the spectrometer. Nowadays, a fairly large list of scintillation phosphors is available with various material parameters, depending upon the individual requirements of the user. Detailed descriptions of the different phosphors are given in the recommended literature cited below. At this point a summary of some important properties is presented for the phosphors which are widely in use nowadays^{379,380,895}. The characteristic data of a scintillation detector are dependent on many parameters of which some are given in Table 4-1.

Tab.4-1: Scintillation phosphor characteristics

Material	Wavelength (nm) ¹	Index of refract. ²	Density (g/cm ³)	Hygroscopic	Conversion efficiency ³
NaI(Tl)	410	1.85	3.67	yes	100
CsI(Na)	420	1.84	4.51	yes	85
CsI(Tl)	565	1.80	4.51	yes	45
CsF	390	1.48	4.11	no	5
⁶ LiI(Eu) ⁴	470-485	1.96	4.08	yes	35
CaF ₂ (Eu)	435	1.44	3.19	no	50
Bi ₄ Ge ₃ O ₁₂	480	2.15	7.13	no	8
BaF ₂	325	1.49	4.88	no	10
TlCl(Be,I)	465	2.4	7.00	no	2.5
KI(Tl)	426	1.71	3.13	yes	24
CaWO ₄	430	1.93	6.062	no	50
CdWO ₄	540	2.3	7.90	no	65
Plastic	350-450	varies	1.06	no	30

¹Wavelength of maximum emission; ²At above named wavelength; ³Referred to NaI(Tl) = 100; ⁴Used for neutron detection

There is also a dependency of the light output rate upon the crystal temperature. This might gain importance in line measurements during industrial processes for product property observations. However, since gamma spectrometry following activation usually is performed at room temperature these data are not

relevant for the present subject. Much more important is the influence of the detector geometry upon the resulting photon spectrum.

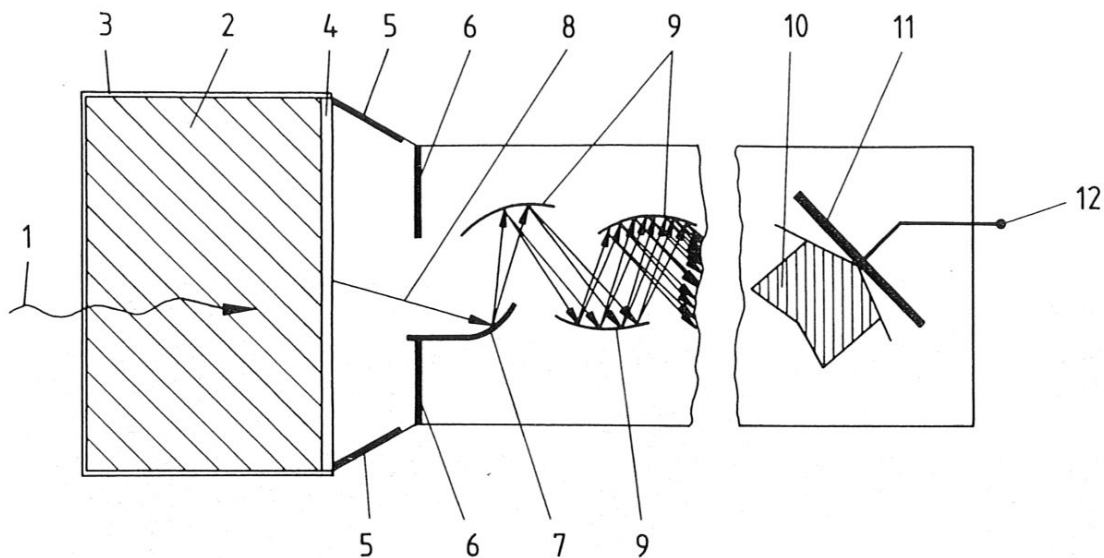


Fig. 4.1: Schematic representation of a scintillation detector; 1 = incident γ -ray, 2 = scintillation crystal, 3 = aluminium detector housing, 4 = photocathode, 5,6,7 = focussing electrode, 8 = photoelectron beam, 9 = photomultiplier dynodes, 10 = electron burst, 11 = charge-collecting electrode, 12 = photomultiplier signal output

There is a large variety of scintillation crystal shapes available so that the analyst is able to select a detector geometry whose performance optimally meets his requirements (see paragraph 4.1.4.7). The geometry presented in Fig.4.2-1 a simple large volume cylinder usually 3 inches high and 3 inches in diameter - is used for standard measurements without special requirements. Low photon energies are measured preferably with a flat crystal, equipped with a thin, low Z element window (usually Be^{381}). This type of crystal is shown in Fig.4.2-4. In Fig.4.2-2 a well-type crystal is presented which serves for quasi - 4π -geometry measurements and finally a horizontally performed well-type crystal (Fig.4.2-3), intended for high efficiency counting of small sample volumes and flow measurements. Using well-type configurations, the integral counting efficiency is significantly improved. However, the appearance of summation signals

(see 4.1.3 below) is also enhanced and therewith the complexity of the resulting spectrum³⁸².

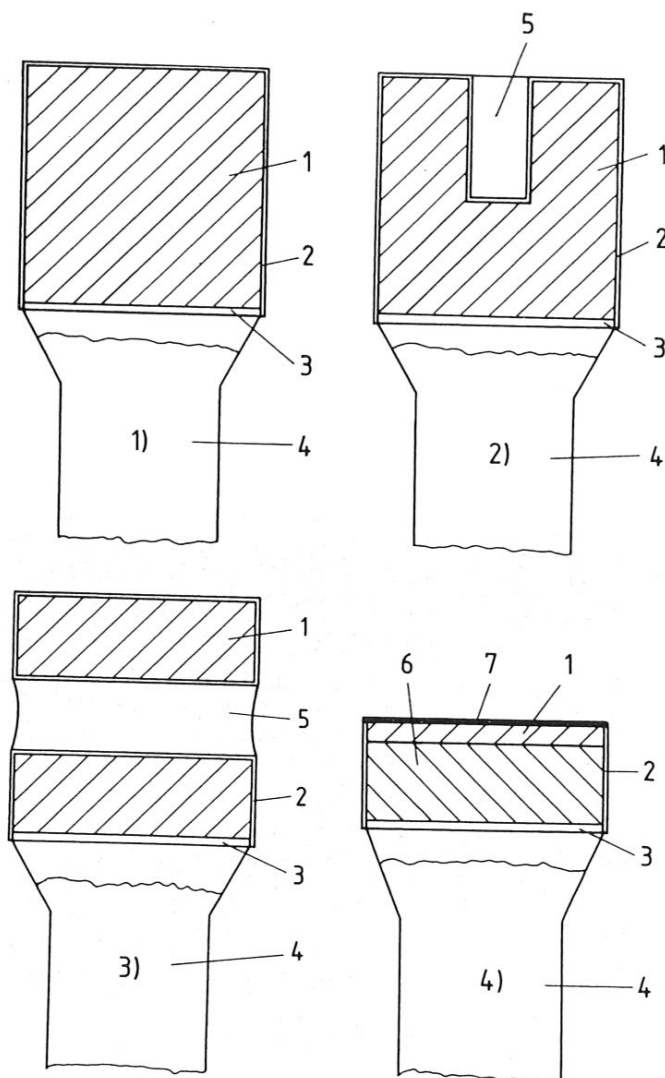


Fig. 4.2: Scintillation crystal geometries; 1 = crystal, 2 = detector housing, 3 = photocathode, 4 = photomultiplier, 5 = well (2) or horizontal drilling (3), 6 = quartz light guide, 7 = beryllium entrance window

As touched on above, the pulses from the photocathode are amplified by secondary electron emission in a photomultiplier tube. The theory and practice of photomultipliers are not evaluated in detail here; it can be taken out of many extended publications³⁸³⁻³⁸⁸. The photoelectrons are focussed on the first of a

series of dynodes, usually fabricated out of Cu-Be alloy sheet material. These electrodes are so arranged that the electrons from each preceding stage are focussed on the next (Fig.4.1). Each dynode of the series is at a potential higher than the preceding one; usually the difference is about 100 volts. This causes the emission of secondary electrons at the next dynode surface. Since the envelope is evacuated there is no electron absorption and a large amplification factor is achieved ranging from 10^3 to 10^{10} . The devices for further pulse processing are discussed in paragraph 4.2.

4.1.2 Semiconductor detectors

The first operating lithium drifted germanium detectors were developed by different working groups in the beginning of the 1960's using the ion drift process suggested by Pell³⁸⁹ (Freck and Wakefield³⁹⁰, Tavendale^{391,392}, Malm et al.³⁹³). The first attempt towards a high resolution detector without usual necessary liquid nitrogen cooling was reported by Maslova et al³⁹⁴.

The first detector geometry was the small planar diode which was abandoned soon in favour of the coaxial geometry, and later reintroduced for low energy photon spectroscopy, especially in the characteristic X-ray energy region i.e. 4-100 keV.

Achievable resolutions and efficiencies rapidly improved. The available active crystal volumes increased from less than one cm^3 of the first detectors to more than 100 cm^3 now. Starting with less than 1% efficiency - compared with a standard NaI(Tl)-crystal - 30 to 40% are not unusual nowadays. The resolution of the first detectors was about 20 keV FWHM (FWHM = full width at half maximum; explanation see paragraph 4.1.4.2) at medium gamma energies; today, a Ge(Li)-detector with a poorer resolution than 2 keV would surely be refused by the purchaser.

Further early and fundamental work about Ge(Li)-detectors was published in Ref's. 394-415, 512, 515, 681.

In the following, semiconductors are discussed which predominantly are used for photon spectroscopy, namely silicon and germanium. Other semiconductor materials which either have been applied for photon counting or are currently in the development stage, are mentioned at the end of this paragraph. The operational principle of a semiconductor detector is comparable to that of an ionisation chamber or a proportional gas counter. The radiation enters an electric-

ally isolating single crystal - usually silicon or germanium - of which two oppositely located areas are used as electrodes to which an operating voltage is connected. If a photon interacts with the detector material, the resulting electrons from photoelectric or other interaction processes will produce a large number of subsequent pairs of electrons and electron defect holes. This cascade process is continued until the electrons have lost their energies insofar as they cannot produce any more charge-carriers. Therefore to a large extent the number of the charge-carriers (and thereby the height of the resulting electric pulse at the output; see Fig.4.3) is exclusively dependent upon the energy of the incident radiation, not upon its kind. This is true since the energy which is necessary to create an electron - electron defect hole pair is independent upon kind and energy of the incident radiation. Also thereby, as is the case in scintillation detectors, the resulting pulse height is proportional to the incident photon energy in the case of total absorption within the detector crystal.

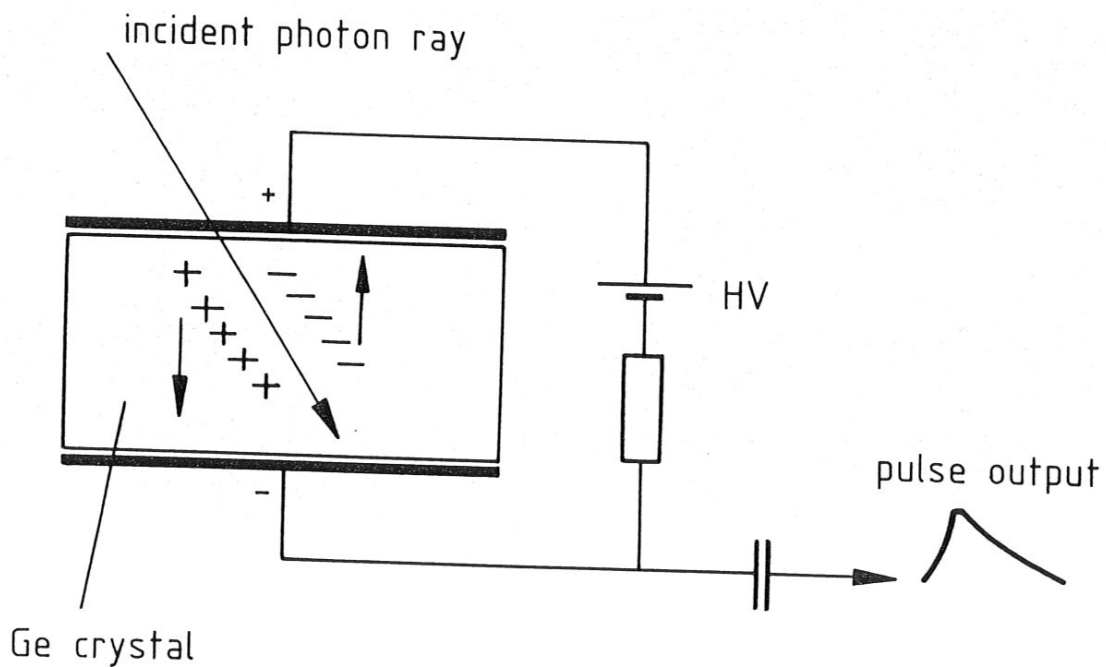


Fig. 4.3: Schematic representation of a semiconductor detector

The most convincing advantage of a semiconductor detector, however, is the excellent energy resolution which can be achieved compared with other detector

systems. This is due to the low mean energy which is necessary to create a pair of charge-carriers within the detector body. The value for germanium is 2.8 eV, for silicon 3.6 eV. In comparison, for the formation of a photoelectron in the photocathode of a scintillation detector, at least 300 eV of radiation energy must be absorbed by the phosphor. Consequently, a much larger number of charge-carriers is produced in a semiconductor detector than in a scintillation crystal of comparable active volume by a photon with a given energy. This means that after exposure to monoenergetic photon radiation the statistical uncertainty of the resulting pulse height is much smaller and the capacity of energy resolution, respectively, is much greater than achievable in scintillation detectors. However, due to unavoidable impurities in the material used for fabrication several significant disadvantages of a semiconductor detector have to be taken into account. At room temperature, an absolutely pure semiconductor crystal is quasi-non-conducting, whereas a "real" crystal has a definite measurable conductivity caused by impurities. Thereby, after application of an operating voltage, a constant current passes the detector and thus the produced electric noise of the crystal leads to severe deterioration of the energy resolution and other properties. There are also other sources of interference, but at this point only the above mentioned one is discussed further, being the most evident one. A way to suppress the interfering conductivity of semiconductor crystals is the implantation of mobile metal atoms, preferable lithium, using the ion drift process reported by Pell³⁸⁹. The theory and practice of the lithium drifting are not discussed here; the reader might refer to the publications in Ref's. ^{397,407,416-427,435,438}.

Nowadays, also intrinsic high-purity germanium detectors are available (actually, drifted crystals are not fabricated any more, as far as the authors could find out inquiring several producers). Due to the extremely high purity of the basic material a compensation of the interfering conductivity through lithium drift is not necessary. The residual conducting impurity can be of p- or of n-type.

Crystals can be configured at various geometries (e.g. coaxial or planar; see Fig.4.4), which result in different properties of the detector behaviour against incoming radiation⁵⁰⁹. Fig.4.4 shows several typical crystal configurations:

Type 1: Intrinsic coaxial p-type high-purity germanium, closed end geometry

Type 2: Lithium-drifted coaxial crystal, closed end geometry

Type 3: Lithium-drifted "true" coaxial crystal, open end geometry

Type 4: Intrinsic coaxial n-type high-purity germanium crystal

Type 5: Well-type crystal, intrinsic high-purity germanium or lithium-drifted

Type 6: Planar crystal

The n-doped contact surface is marked black.

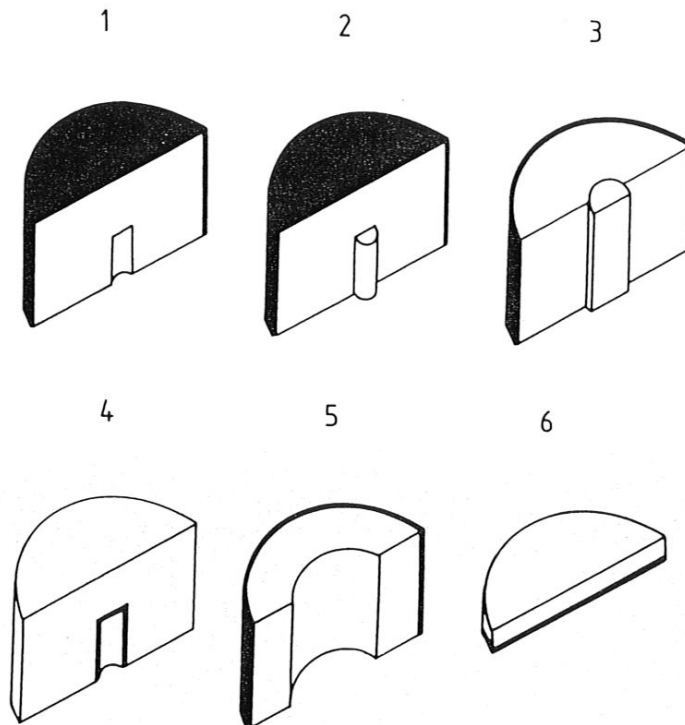


Fig. 4.4: Semiconductor crystal configurations; explanations see text

Therefore, both different drift configurations and detector shapes favour the measurement of different radiation energies. Generally planarly drifted crystals have better energy resolutions whereas coaxially drifted ones, due to greater achievable active volumes, offer larger efficiencies and peak-to-Compton ratios (see Fig. 4.5). These parameters are explained in detail in paragraph 4.1.4. For the detection of low energy photons it is important to keep the thickness of the inactive entrance layer as low as possible. This can be achieved using the configurations of types 4 and 6, respectively, in Fig. 4.4.

As noted above, Si and Ge single crystals are primarily used as detector materials. Si-detectors are useful for the detection of very soft photon radiation (see Ref's. ^{397, 413, 428-434, 436, 437, 513, 674}) - in this case the detector housing is equipped with a thin (several tenths of millimeters) beryllium window to al-

low the access of soft radiation to the detector crystal - whereas, due to its higher atomic number, germanium detectors are more suitable for spectroscopy of higher gamma energies (see Fig's.4.6 and 4.7).

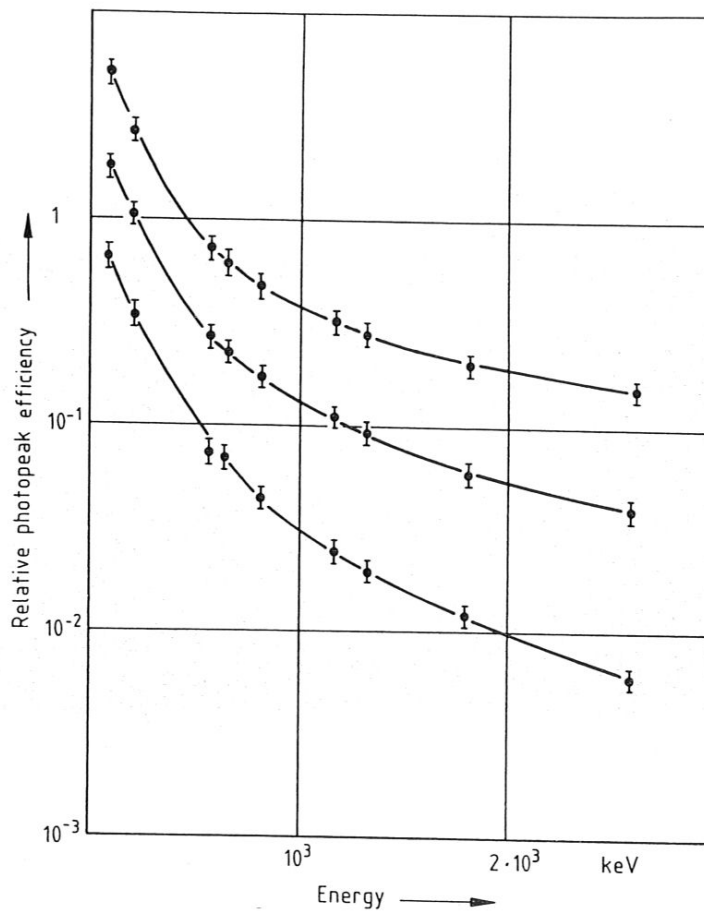


Fig. 4.5: Relative full energy peak efficiency as a function of the measured energy; upper curve: five-sided crystal, middle curve: "true" coaxial crystal, lower curve: thin planar crystal; explanations see Fig.4.4 and paragraph 4.1.4.3

For different reasons, germanium and silicon photon detectors have to be cooled down to a temperature of about -200°C during operation. This is done by a cryostat with liquid nitrogen (see Fig.4.8). The necessity of the cooling entails the requirement of considerably large space for storage and poor mobility of the spectrometer. While lithium drifted silicon detectors - if not connected to

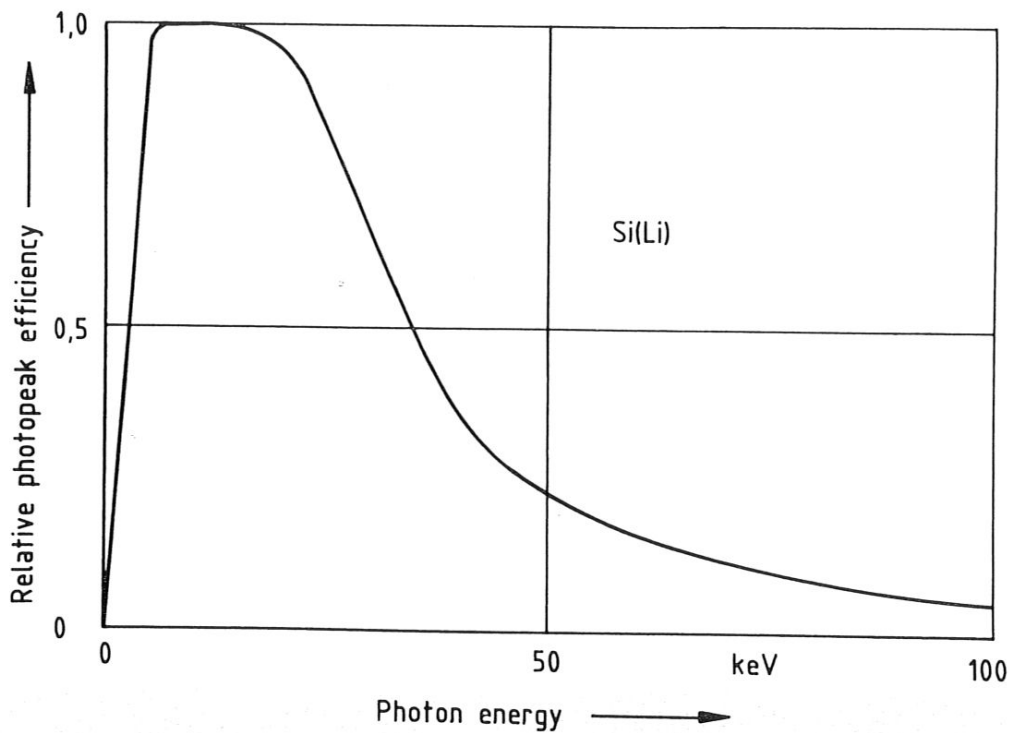


Fig. 4.6: Relative full energy peak efficiency of a lithium-drifted silicon detector as a function of the measured photon energy; explanations see paragraph 4.1.4.3

the operating voltage - may be stored at room temperature, drifted germanium detectors have to be continuously cooled to avoid the drifting of the lithium out of the detector body onto the crystal surface which would cause severe damage of the detector. Intrinsic high-purity germanium detectors may be stored at room temperature as long as they are not connected to the operating high voltage. Further information about the property and performance of high-purity germanium detectors can be found in Ref's. 439-442.

Effort has been directed from the very beginning of the development of semiconductor detectors towards finding a material which allows high resolution photon spectroscopy without cooling of the crystal in order to ease the handling of the detector and enhance the mobility of the spectrometer, so that the analyst is enabled to perform "on-site" measurements, for instance, in geological prospecting. Most of the semiconductor detector manufacturers offer portable cool-

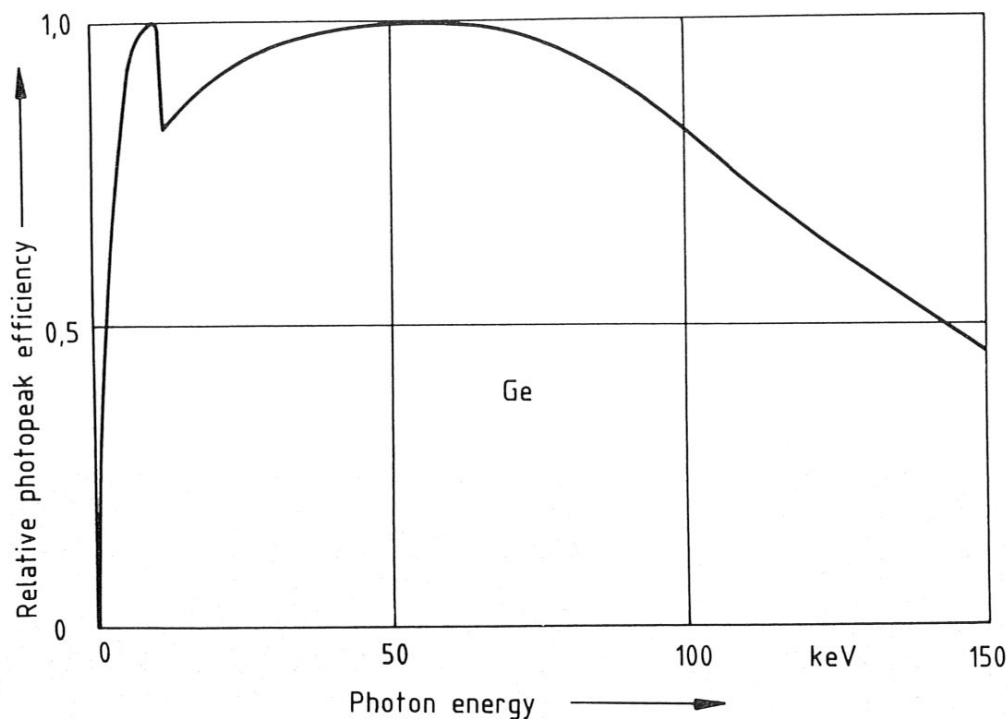


Fig. 4.7: Relative full energy peak efficiency of a planar germanium detector as a function of the measured energy; explanations see paragraph 4.1.4.3

ed detectors equipped with small liquid nitrogen Dewar vessels (see Fig.4.9), but due to the relatively small Dewar containers their field-period is limited.

Several alternative materials have been suggested and intensively studied, e.g. CdTe, HgI₂ and high purity Si; even natural diamonds have been studied^{443,444}. See also Ref's. ^{335,445-477,895}. Among them, HgI₂ appears to be most promising in its performance. An extended review on HgI₂ as a semiconductor detector material was given by Schieber⁴⁶⁴. However, photon activation analysis generally is carried out in the laboratory and so one is hardly confronted with a question of mobility of the spectrometer and therefore uncooled high resolution detectors are not discussed further here. Moreover, the development of these seems to be still in the prematurity stage and there will be required a lot of further research work until their state of maturity is reached. As far as the authors know, no other high resolution detector system is commercially available as yet which offers performance comparable to that of conventional detectors and does not require any cooling. Anyway, it is an interesting development

worthwhile keeping track of.

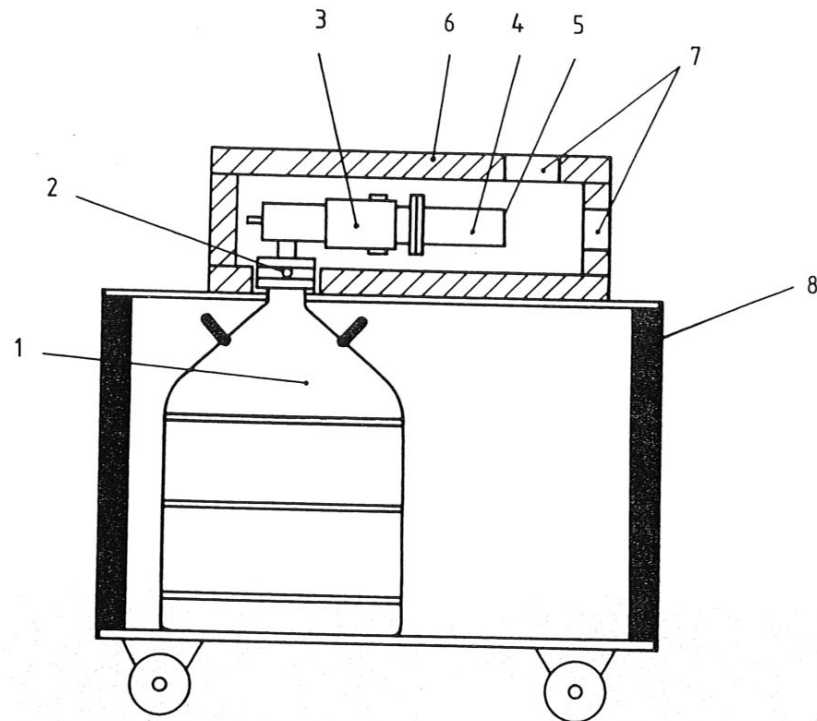


Fig. 4.8: Ge(Li)-detector setup; 1 = Dewar vessel, 2 = inlet for liquid nitrogen supply, 3 = preamplifier, 4 = detector housing, 5 = sample position, 6 = lead shielding, 7 = sample inlet, 8 = detector carriage

The performance of germanium high resolution spectrometers are discussed further in detail in the paragraphs 4.1.4, 4.3 and 4.4.

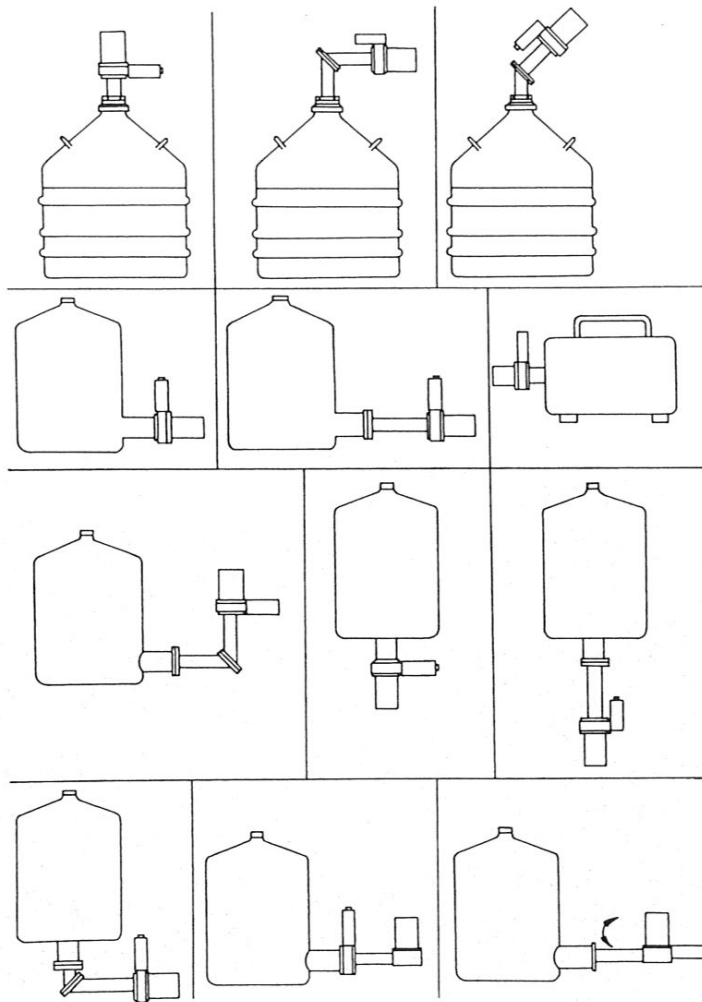


Fig. 4.9: Cryostat configurations of semiconductor photon detectors

4.1.3 The pulse amplitude spectrum

At this point the different contributions to the photon spectrum are discussed. This is done somewhat in detail since it is of importance for the understanding and proper interpretation of the photon spectra in activation analysis. In Fig.4.10 all effects giving rise to electric pulse signals are presented schematically.

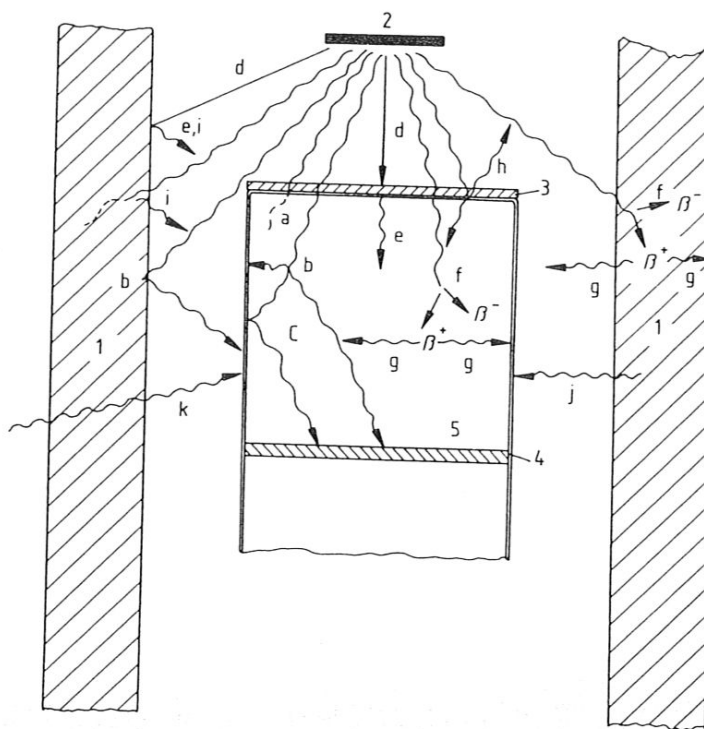


Fig. 4.10: Effects registered in a scintillation γ -ray detector; 1 = lead shielding, 2 = radiation source, 3 = β -absorber, 4 = photocathode, 5 = scintillation crystal

a: completely absorbed photon ray (by photoeffect or other mechanism), b: scattered γ -ray (Compton scattering), c: examples of different paths of the luminescence light, d: β -ray, e: bremsstrahlung, f: pair production and subsequent positron annihilation, g: annihilation quanta, h: escaping characteristic X-ray radiation of the detector material, i: X-ray fluorescence of the shielding material, j: radiation due to radioactive impurity in the shielding material, k: external radiation penetrating the shielding

The path of the luminescence light is shown only for the case of Compton interaction (c)

It can be seen that various influences upon the detector signals are due to the radiation shielding. Therefore, in practice, it is of advantage to either keep a large distance between the shielding and the detector housing or, if this is - presumably by lack of space in the laboratory - not possible, to provide an "inner" shielding layer of lower atomic number material (e.g. Cu or Fe).

Thereby excessive background radiation due to X-ray fluorescence in the lead is avoided. All described kinds of interaction of photons with matter produce detectable signals in both scintillation and semiconductor detectors. The shape of the pulse height spectrum is different for both detectors (see Fig. 4.11); it is firstly dependent upon the above described essentially different function principles and secondly upon the different physical properties and material parameters of the crystals.

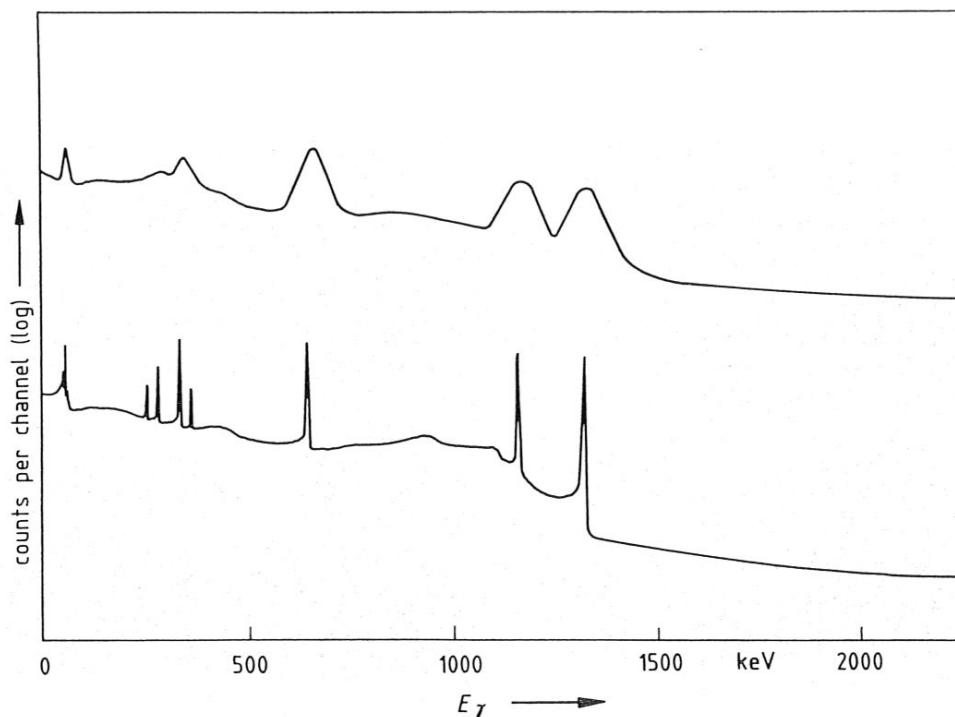


Fig. 4.11: NaI(Tl)- (upper curve) and Ge(Li)-spectrum of ^{133}Ba , ^{137}Cs and ^{60}Co

This is specified in paragraph 4.1.5. The diagrams in Figs.4.12 and 4.13 indicate which of the various kinds of interaction dominates in the detector material at a given photon energy. In Fig.4.14 the pulse height spectrum of a low energy gamma emitting radionuclide measured with a 3" by 3" NaI(Tl) detector is represented (^{241}Am ; $E_\gamma=60$ keV). It can be derived from Fig.4.12 that this energy is absorbed almost entirely by the photoelectric effect. Therefore the spectrum is quite simple. The smaller peak at the low energy side of the photoeffect signal (also called "photopeak") is due to escape of characteristic iodine X-radiation from the detector surface (see Fig.4.10). Along with increasing photon energy the pulse height spectrum becomes more complicated. In Fig.4.15 a gamma-ray spectrum of a medium-energy emitter is shown (^{51}Cr ; $E_\gamma=320$ keV).

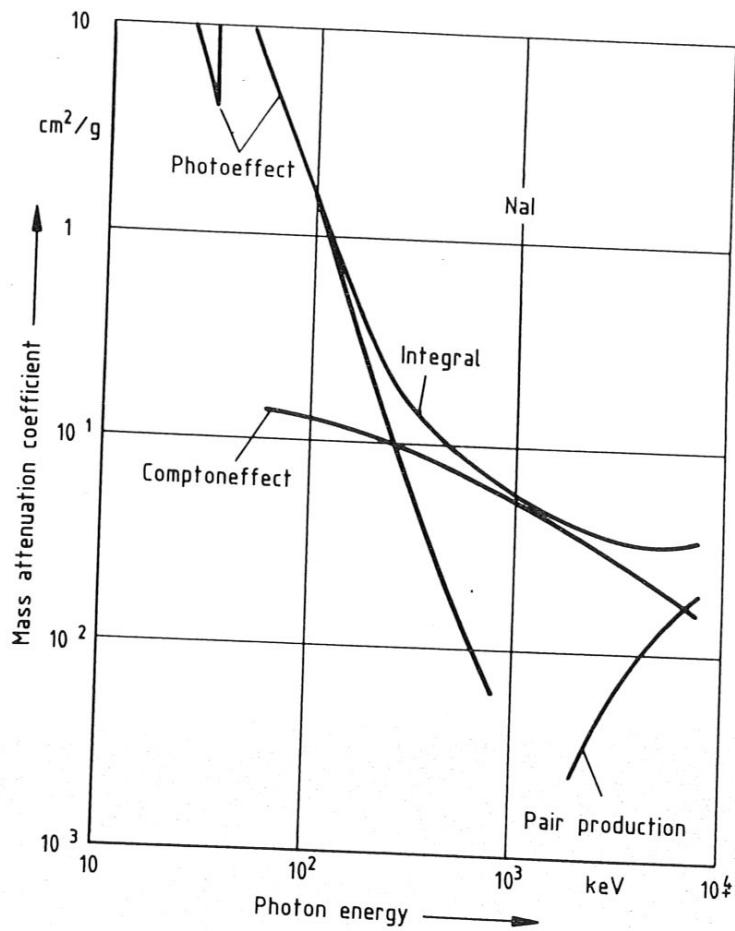


Fig. 4.12: Mass attenuation coefficient of NaI as a function of the photon energy

Inspection of the NaI absorption cross section function in Fig.4.12 indicates that these gamma-rays will interact with the detector material by both Compton scattering and photoelectric effect. Theoretically the spectrum should contain a monoenergetic line and a Compton continuum with a sharp cut-off at an energy somewhat below the photopeak (see Fig.4.16, dashed line). In the measured spectrum the photopeak appears as a rather broad, quasi-Gaussian function which is not clearly separated from a Compton continuum. This shape is both due to fluctuations in the light yield of the radioluminescence of the phosphor and also due to statistically occurring processes in the photomultiplier operation. Moreover, comparison between the theoretical and the actual spectrum indicates

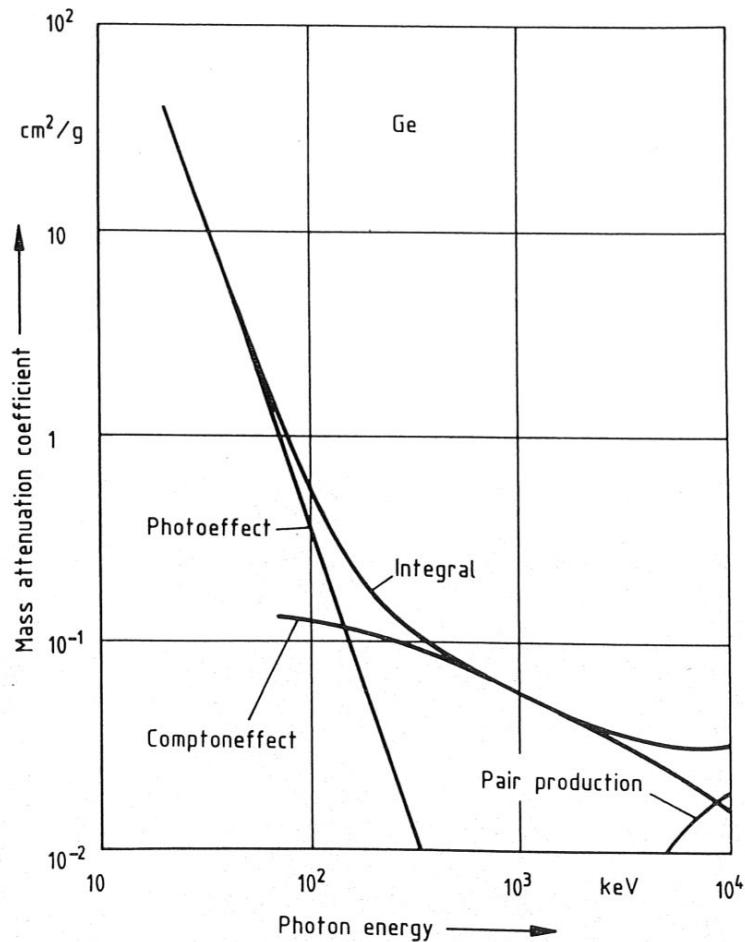


Fig. 4.13: Mass attenuation coefficient of germanium as a function of the photon energy

a significantly higher photopeak compared with the Compton continuum height. This is due to the quasi-prompt absorption of Compton-scattered photons within the crystal. Thus a full energy transfer is achieved and a signal representative for this energy is created and passed on to the following spectrometry units. A Compton signal is created in the case of escape of the scattered photon from the detector crystal. With further increasing gamma-ray energy, the fraction of pulses in the photopeak is reduced compared with the Compton electron continuum (Figs. 4.16 and 4.17; 835 keV from ⁵⁴Mn). Since in this energy region the Compton effect becomes more dominant (see Fig. 4.12). Backscattered gamma-rays due to scattering in the detector surroundings are detected in the lower energy region of the spectrum (see Fig. 4.10). Yet more complicated the

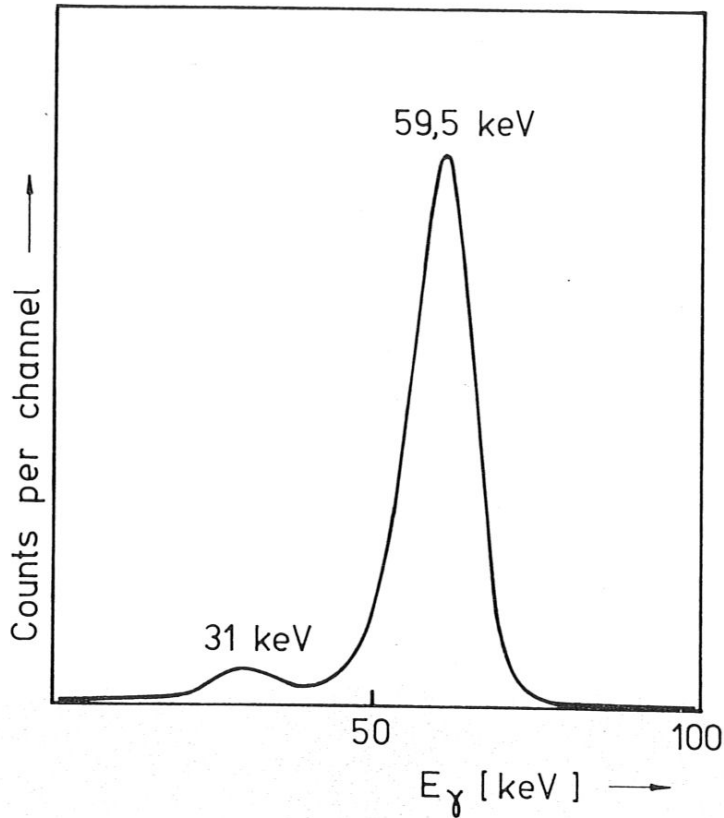


Fig. 4.14: γ -ray spectrum of ^{241}Am taken with a sodium iodide detector

spectrum becomes when energies above 1022 keV are measured (Fig.4.18; ^{28}Al). In addition to the photopeak and the Compton electron distribution several satellite peaks are superimposed upon the Compton continuum as a result of interaction by pair process. First, as also observed in the ^{54}Mn spectrum in Fig.4.17, a peak due to backscattering in the material in the close neighbourhood of the detector appears. Then, by annihilation of the positron which - together with an electron - was created by the pair production process occurring in the detector shielding material, a peak at the pulse height location representing 511 keV is visible. As explained above, at the total incident photon energy minus 1022 keV a peak is detected (double escape line due to escape of both 511 keV quanta from the detector) and also a single escape line which appears due to escape of one of the 511 keV quanta pair. Finally, the full incident energy signal, the photopeak, is present as the distinguishing characteristic of all

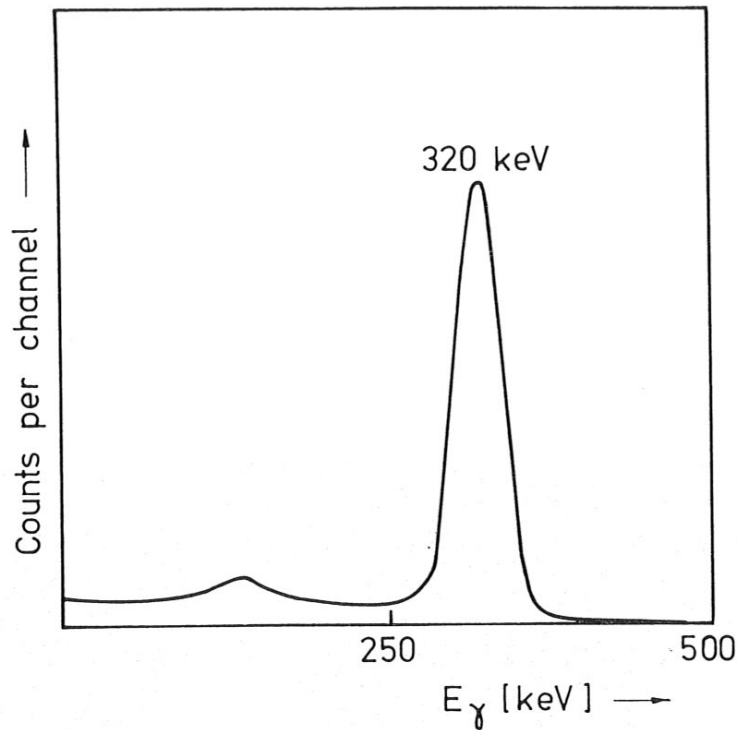


Fig. 4.15: γ -ray spectrum of ^{51}Cr taken with a sodium iodide detector

gamma-ray spectra.

Besides, as will be explained later and also is touched on in Ch.2, the 511 keV peak will almost always be the most prominent in a gamma-ray spectrum after photon activation, due to the nature of the majority of the product nuclides; positrons can be emitted by photonuclear reaction products and also through pair production during absorption of high-energy gamma quanta in material in the close neighbourhood of the detector.

Besides the above mentioned signals due to Compton scattering outside the detector, other radiation signals might be observed which originate in the detector environment (see Fig.4.10). Bremsstrahlung may be produced by beta absorption both in the lead shield and the detector housing and also characteristic lead X-rays caused by photoeffect interaction in the lead shielding and/or fluorescence excited by beta radiation.

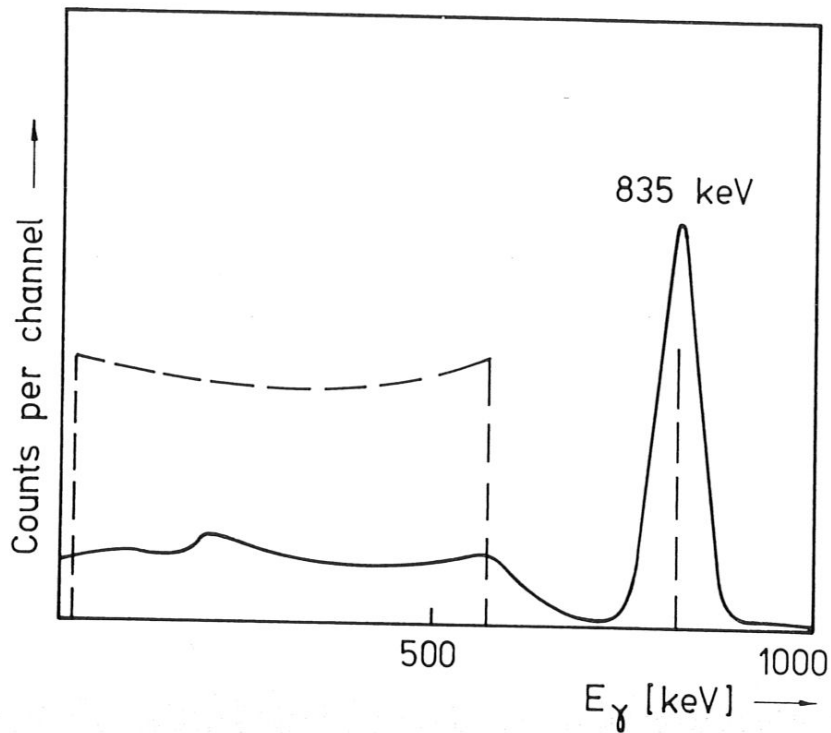


Fig. 4.16: γ -ray spectrum of ^{54}Mn (NaI-detector); dashed line: theoretical pulse height distribution

Finally, summation effects give rise to additional signals. If two events occur within the time resolution limit of the detector, e.g. the light emission lifetime of the phosphor in a scintillation detector, the analog pulse in this instance will represent the sum of the energies transferred to the detector by both quasi-simultaneous events (see Fig.4.19). This effect is most probable in the case of cascade emission of gamma-rays by the measured radionuclide, but may also occur by other mechanisms of more random nature (Heath⁴⁷⁸). The summation probability is significantly enhanced if well-type detectors for quasi- 4π -geometry counting are used (see Fig.4.2b). In figure 4.19 spectra are normalised to equal net area of the full energy peak doublet. The enhancement of the summation effect in the case of well-type counting can be demonstrated by calculating the ratio between the sum peak net areas and the common full energy signal doublet net area mentioned above; in the case of plain crystal counting this ratio was found to be 0.0265; in the case of well-type counting it was 0.126, i.e. larger by a factor of 4.75. Most favoured, however, is the summation effect if 511 keV annihilation radiation is counted in a well-type detector

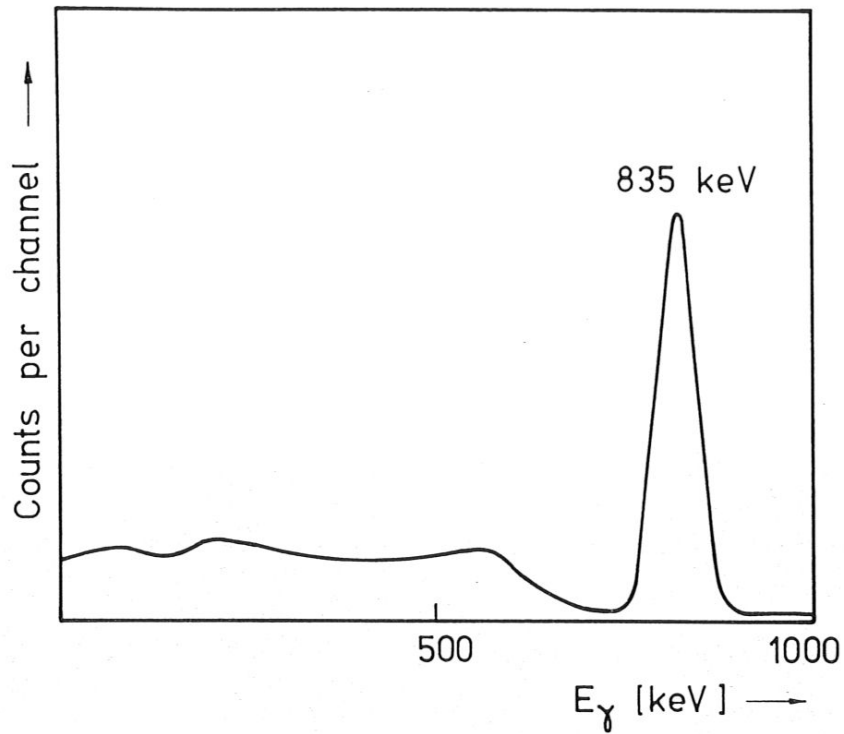


Fig. 4.17: γ -ray spectrum of ^{54}Mn taken with a sodium iodide detector

because two annihilation quanta are emitted simultaneously. Therefore, the 1022 keV summation line will be one of the most prominent in a spectrum containing annihilation radiation if taken in well-type geometry.

The appearance of the various satellite peaks mentioned above within a gamma-ray spectrum containing high-energy lines is demonstrated in Fig.4.20.

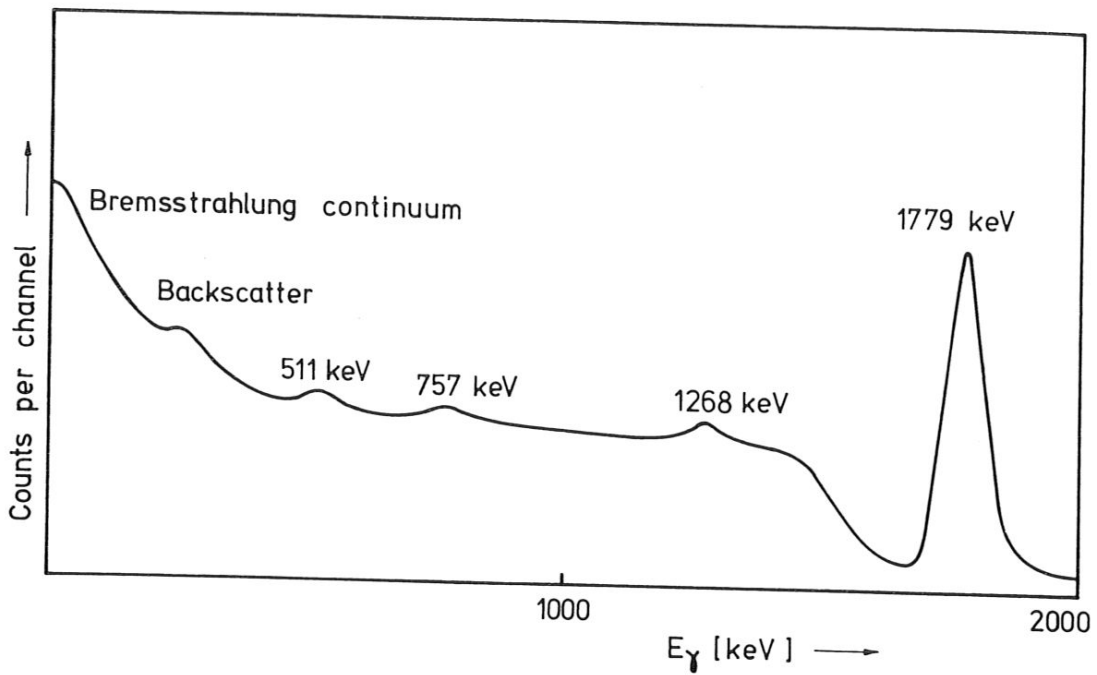


Fig. 4.18: NaI-spectrum of ^{28}Al ; 757 keV and 1268 keV: escape peaks

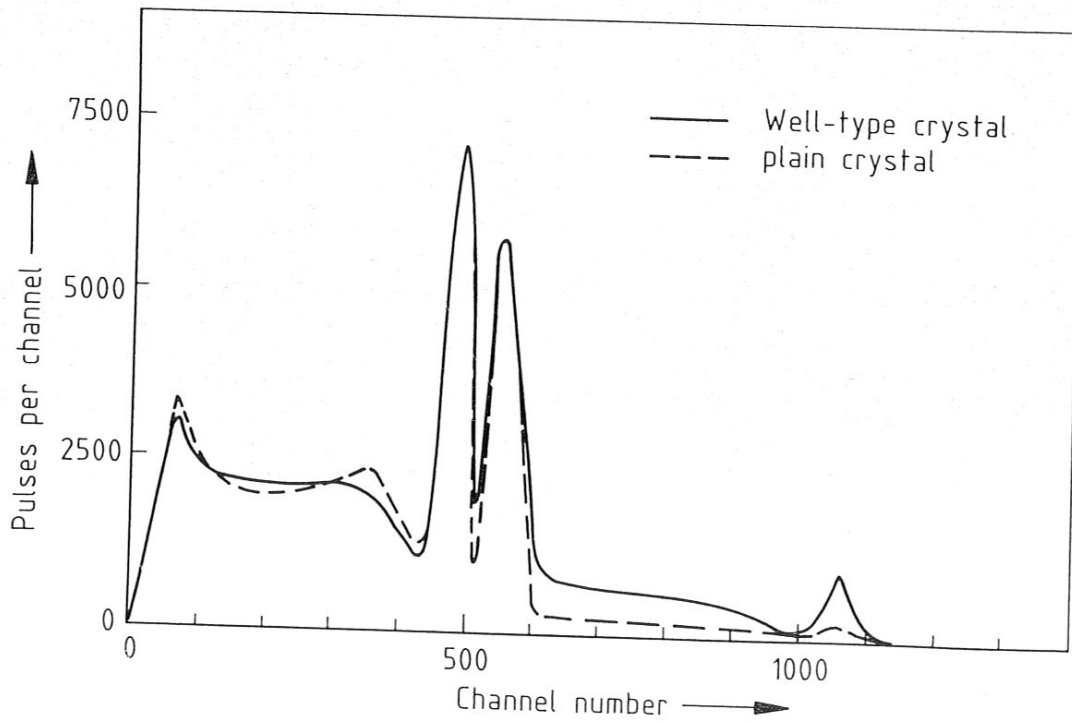


Fig. 4.19: ^{60}Co -spectrum taken with a plain (dashed line) and a well-type NaI-detector; the pulse numbers are normalised to a common maximum at 1173 keV.

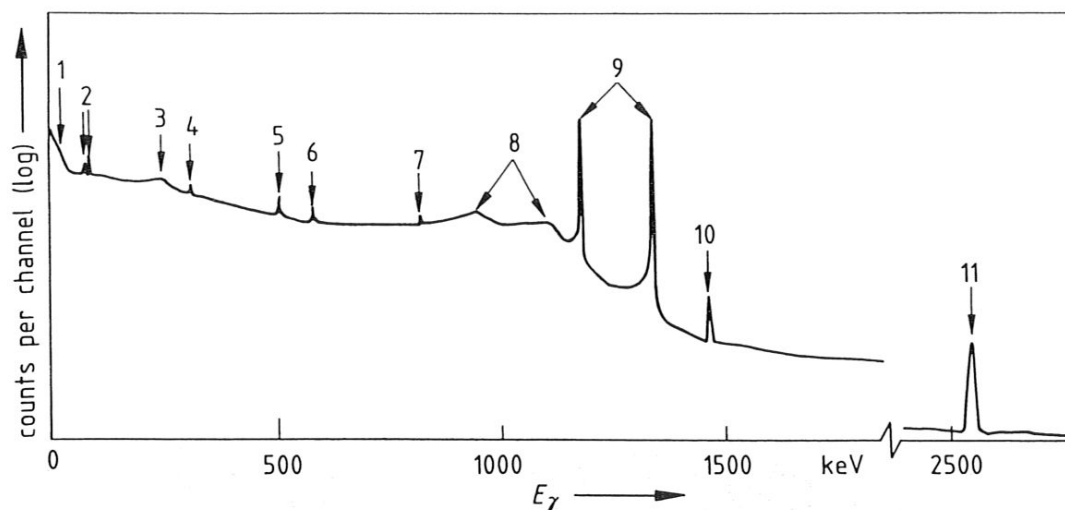


Fig. 4.20: γ -ray spectrum of ^{60}Co taken with a large-volume Ge(Li)-detector; 1 = bremsstrahlung continuum, 2 = X-ray fluorescence of lead (by radiation interaction with the shielding material), 3 = backscattering peak (Compton scattering in the shielding), 4 = not identified (possibly radioactive impurity in the shielding), 5 = 511 keV annihilation radiation signal (pair production in the shielding), 6,7 = escape peaks (pair production in the crystal), 8 = Compton edges (due to both γ -energies), 9 = full energy signals, 10 = γ -ray energy emitted by ^{40}K (1461 keV penetrating the lead shielding), 11 = peak due to summation of both γ -energies, absorbed quasi-simultaneously (2506 keV)

4.1.4 Relevant characteristics of detectors

At this stage, intrinsic properties of a detector are discussed. Both detector systems (scintillation crystal and semiconductor detector) are compared. Integral efficiencies, resolution etc. of a spectrometer can be enhanced, of course, by improved electronic equipment and special counting arrangements, e.g. anti-Compton spectrometry; this is discussed in the paragraphs on the spectrometry electronics below. The detector characteristics which are relevant for activation analysis are:

- a) the practical maximum measurable count rate
- b) the energy resolution
- c) the photopeak counting efficiency
- d) the signal-to-Compton continuum ratio
- e) the linearity of the energy versus pulse height function
- f) the energy limits of the measurable photon spectrum
- g) generally available crystal geometries

and some additional more general data like purchase price, space requirement etc.. These are summarised in Tab.4-2 below. Some of the above listed characteristics influence each other and therefore, in selecting an adequate detector for a given task the analyst has to find an optimum between the properties to meet his special requirements. As clearly shown in chapter 2, the majority of the product nuclides after bremsstrahlung activation emit a very intense characteristic X-ray spectrum which - as demonstrated in paragraph 4.1.2, Figs.4.6 and 4.7 - most advantageously is measured with help of planar semiconductor diodes equipped with a thin beryllium window. Therefore, in the following, these spectrometers will be discussed separately in each relevant case.

4.1.4.1 Maximum measurable count rate

This is a function of the time resolution of the spectrometer. It is dependent upon many parameters, e.g. the way in which the electric pulse is created, the detector size and geometry, the quality of the detector material and, last not least, the quality of the pulse processing electronic system. It is primarily influenced by the shape of the electric pulse (rise- and decay time, pulse height etc.). In semiconductor detectors it is limited by many parameters since the pulse production process is very complicated and strongly influenced by the electronic noise of the crystal⁴⁷⁹. The time resolution of a scintillation crystal detector is primarily determined by the decay time of the fluorescence

light which is comparably short. Therefore, relatively high count rates can be achieved with a scintillation detector without signal deterioration of the photopeak shape, whereas high pulse rates, when measured with a semiconductor detector of comparable active volume, entail serious loss of energy resolution capability of the spectrometer. As noted above, by special electronic processing devices connected to a semiconductor detector one can, within limits, process also high count rates satisfactorily. This is discussed further in paragraph 4.2 on the electronic pulse processing systems. The functions in Fig. 4.21 were measured under fixed conditions (^{137}Cs point source; $E_\gamma=662$ keV; 10 cm distance from the detector housing) using standard pulse processing electronics without special arrangements like pile-up rejector, high-performance base line stabiliser etc.. The units of the resolution data which are plotted over the count rate are explained and discussed further in the following paragraph on the energy resolution. The different dead-times of the crystals (scintillation or semiconductor) are not discussed here since the major source of dead-time within a photon spectrometer is due to the analog-to-digital converter of the multichannel analyser (see paragraph 4.2.3).

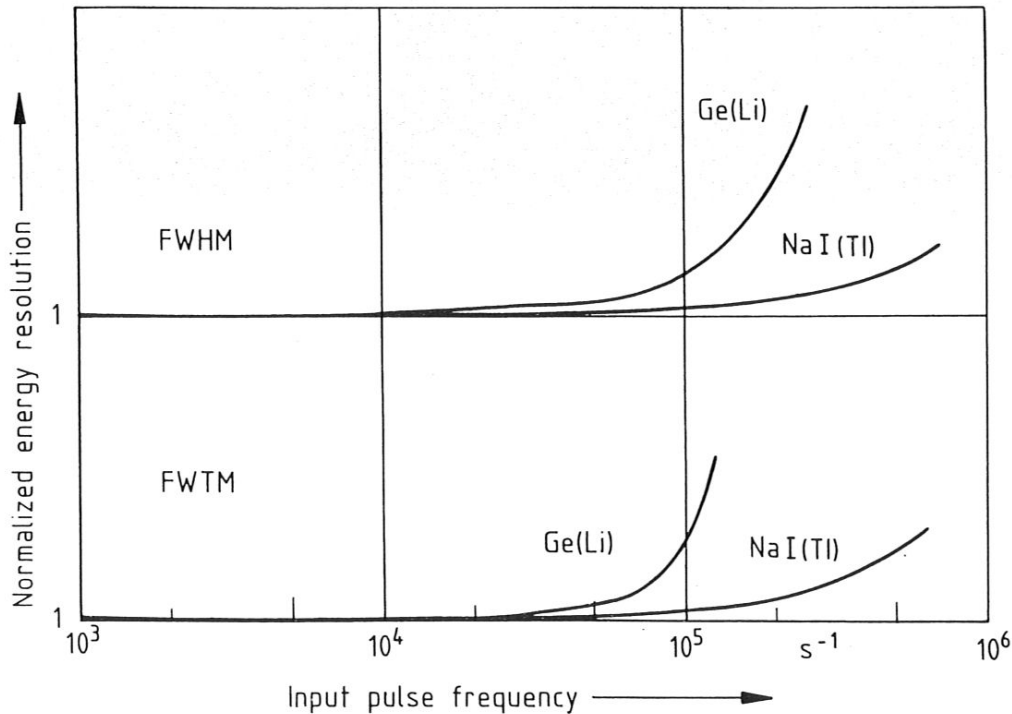


Fig. 4.21: Peak resolution of a γ -spectrometer (NaI/Ge) as a function of the count rate

4.1.4.2 Energy resolution

As touched on above the most evident difference between the detector systems discussed here are the achievable energy resolution capabilities. By comparison of the spectral performances (see Fig.4.11) it becomes evident that this difference makes the decision between both detector types in the case of instrumental multielement activation analysis.

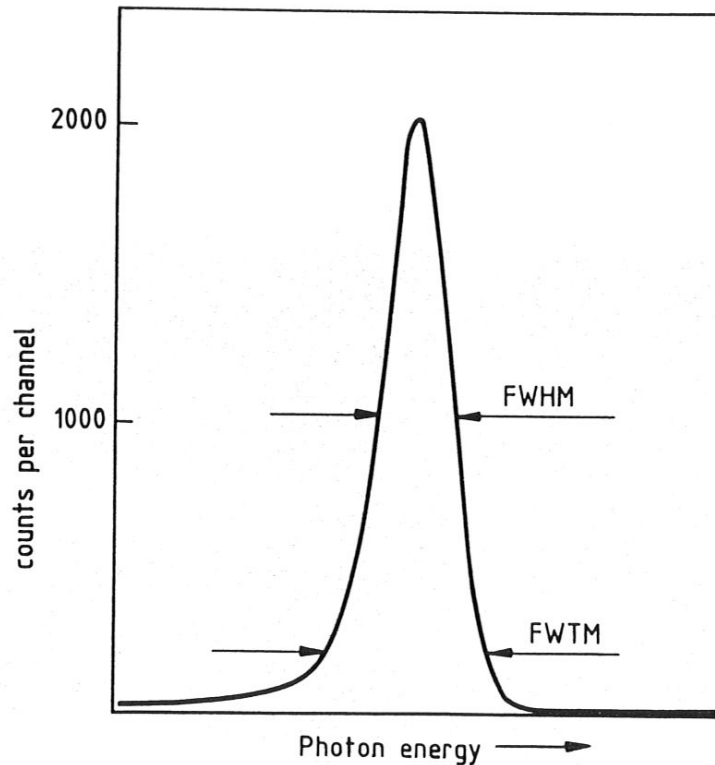


Fig. 4.22: Peak resolution parameters; FWHM = full width at half maximum, FWTM = full width at tenth maximum

One distinguishes between the absolute and the relative photopeak energy resolution. The absolute one is given as full width of the photopeak at half its total net height (full width half maximum = FWHM, given in keV). Another important aspect concerning the detector resolution performance is the photopeak width at a tenth of its maximum, i.e. close to the background line (full width tenth maximum = FWTM). This value reflects the peak shape (see Fig.4.22). The

relative energy resolution is given by:

$$R = \frac{\text{FWHM}}{E_{\text{Ph}}}$$

$$R = \frac{\text{FWTM}}{E_{\text{Ph}}}$$

respectively, where E_{Ph} is the photon energy. This implies that both the absolute and the relative resolution are dependent upon the energy of the measured photopeak (see Figs. 4.23 and 4.24).

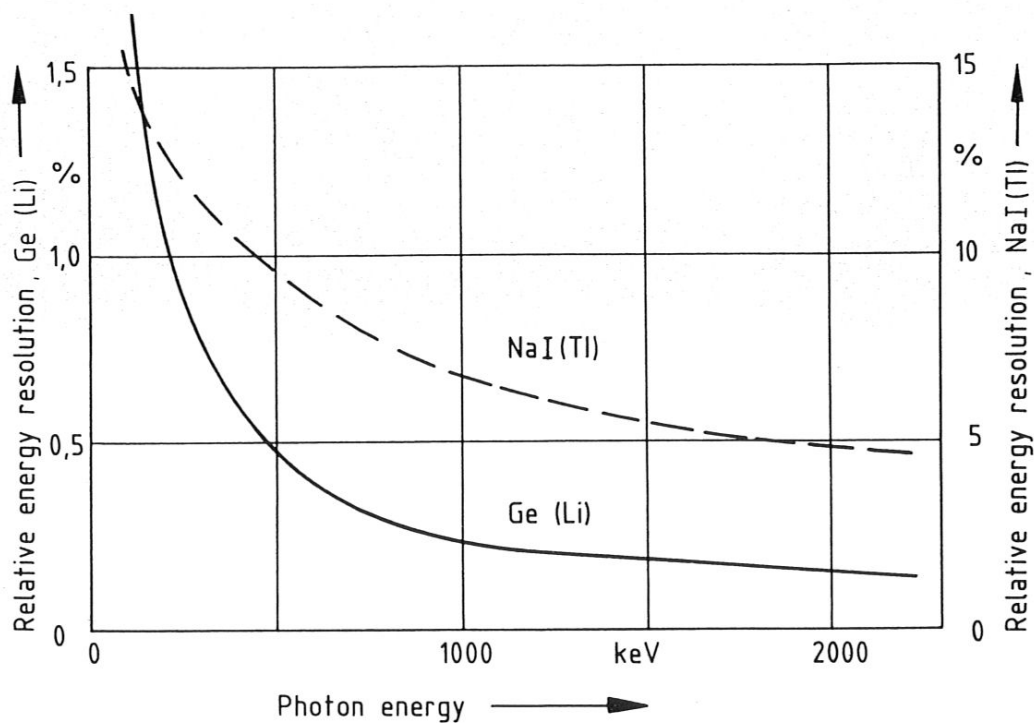


Fig. 4.23: Relative full energy peak resolution as a function of the measured energy

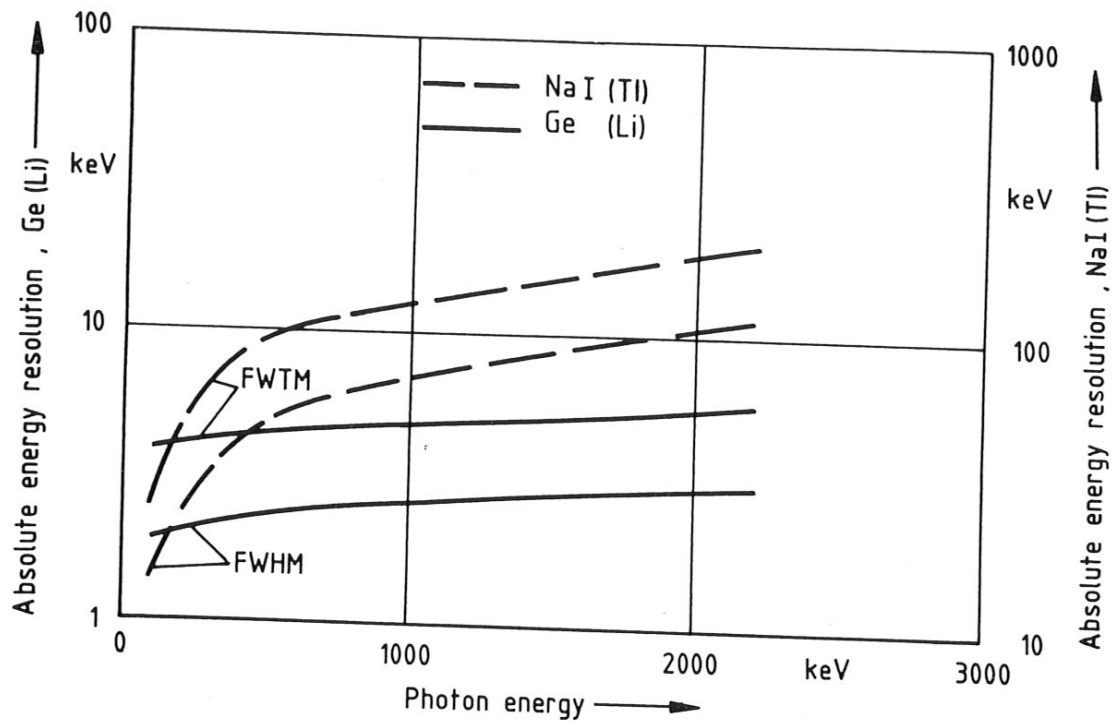


Fig. 4.24: Peak widths produced by a γ -spectrometer at full energy absorption as a function of the measured energy (absolute resolution)

At higher incident photon energies more charge carriers are produced within the active detector volume during total energy absorption to yield a larger analog electric pulse at the signal output. The relative uncertainty of the number of charge-carriers in this case is smaller, and therefore, the relative energy resolution is better; it thus improves with the photopeak energy (see Fig.4.23). On the other hand, at higher number of charge carriers created along the path of the incident photon the absolute uncertainty of their number increases and, along with it, the absolute energy resolution of the detector, expressed as FWHM or FWTM (see Fig.4.24) is degraded. Caused by statistical reasons, the increase of the peak width of scintillation detectors is much more pronounced than is the case in semiconductor detector spectra. This is another advantage of semiconductor detectors in the case of complex photon spectra to be measured. The energy resolution - as one of the most relevant technical data of a detector - is given in the accompanying data sheet or certificate in the same consensus units in all cases by all detector manufacturers; this way of presentation is summarised for all relevant data and presented in paragraph 4.3.

As mentioned above, low energy photon spectrometry has found widespread application in activation analysis, particularly in photon activation analysis (see Ch's. 2 and 6). Planar silicon or germanium diodes are used for low energy photon measurement (see Fig. 4.25).

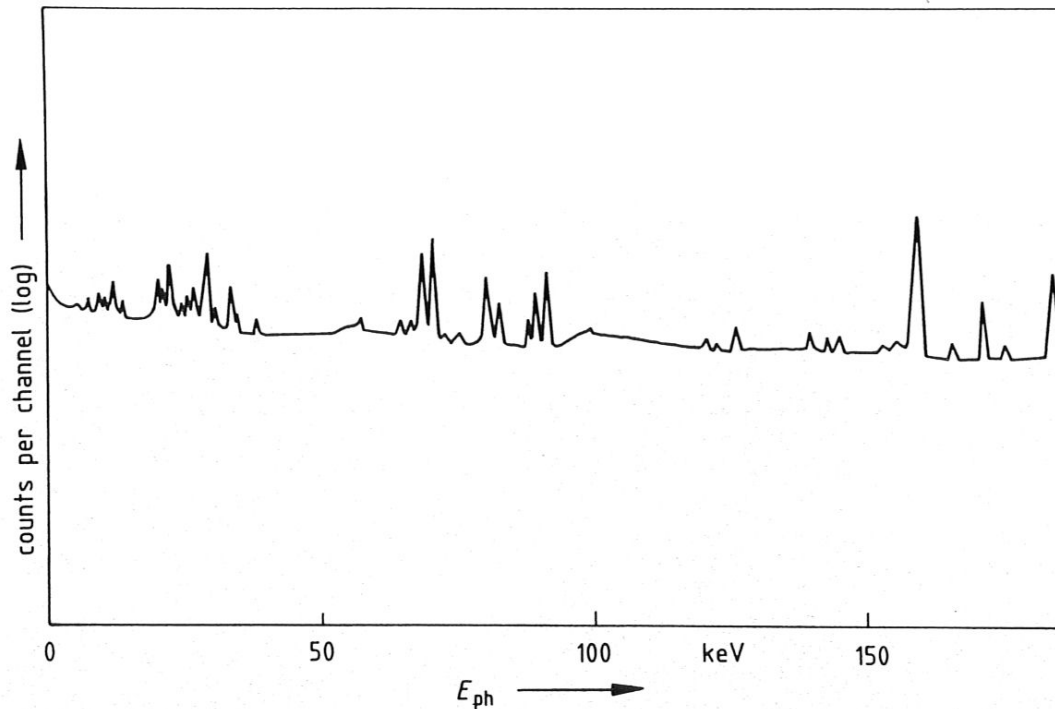


Fig. 4.25: Multi-component spectrum taken with a planar low energy photon diode

As noted above, these relatively small detector crystals have considerably better energy resolution capabilities than larger coaxial ones. However, as is the case in scintillation detectors, the absolute resolution capacity rapidly decreases with increasing incident photon energy (see Fig. 4.26). Anyway, their resolution performance is brilliant and therefore they are especially suitable for characteristic X-ray spectra measurements (see Fig. 4.25). One disadvantage of low energy photon spectroscopy is the strong self-absorption of the soft radiation within the sample. Therefore, one has to follow special precautionary measures to prevent erroneous data evaluation. This is discussed further in the description of practical cases in the applications section in chapter 6.2.

For more information about the intrinsic resolution capacity of detectors, semiconductor crystals in particular, the reader might refer to the literature in

Ref's. 480-484.

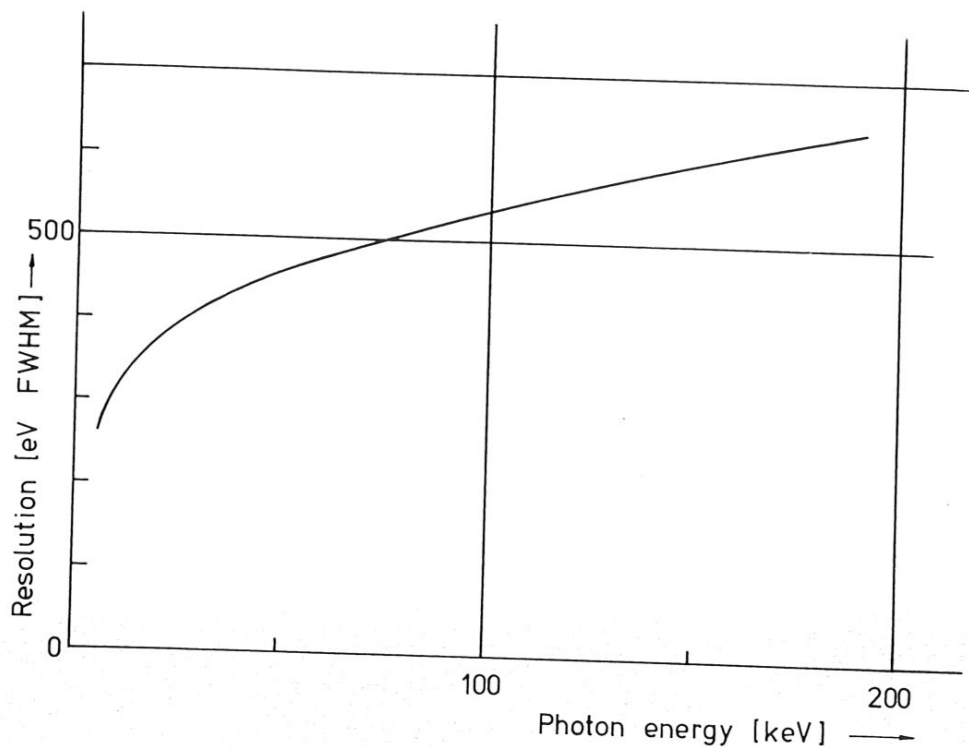


Fig. 4.26: Absolute energy resolution of a planar low energy photon germanium diode as a function of the photon energy.

4.1.4.3 Full energy peak counting efficiency

This is the ratio between the total photon emission rate of the source to be measured and the pulse rate collected within the photopeak area of the spectrum, or, expressed otherwise, the probability that an emitted photon is completely absorbed by the detector. As explained in the preceding paragraph, a pulse whose height is representative for the energy of the incoming photon is created if its energy is transferred entirely to the electrons of the active partition of the detector crystal material. This has to occur within a sufficiently short time period to produce a distinctly processible electric signal. Hence, several parameters are responsible for the photopeak counting efficiency of a detector (the exact term, as indicated in the headline of this paragraph, is "full energy peak" rather than "photopeak", which is commonly used for its shortness' sake. The full energy signal can be produced both by primary full photon energy transfer to the detector crystal (photoeffect) and by Compton

scattering and subsequent absorption of the scattered photon by the crystal within a sufficiently short time as mentioned in paragraph 4.1.3).

Most naturally, the counting efficiency is very much dependent upon the counting geometry, i.e. the distance of the source from the detector and the shape of the radiation source (e.g. point- or extended area geometry)⁴⁸⁵. An algorithm for the measurement of the counting efficiency using different source geometries is given by Heath^{478,486}. Using a well-type crystal configuration, radiation can be counted most efficiently since its isotropical distribution is exploited with a quasi- 4π -counting geometry, but, as already noted, entails drawbacks which will be specified later on. The counting efficiency decreases along with the square of the distance, if the source is not very close to the detector crystal. In this case some other geometrical parameters influence the function (see paragraph 4.4). There is no significant intrinsic difference in the efficiency behaviour of scintillation and semiconductor detectors against the counting and source geometry. This also - to a certain extent - applies to another factor which takes influence upon the efficiency, namely the energy of the incident radiation (Fig.4.27).

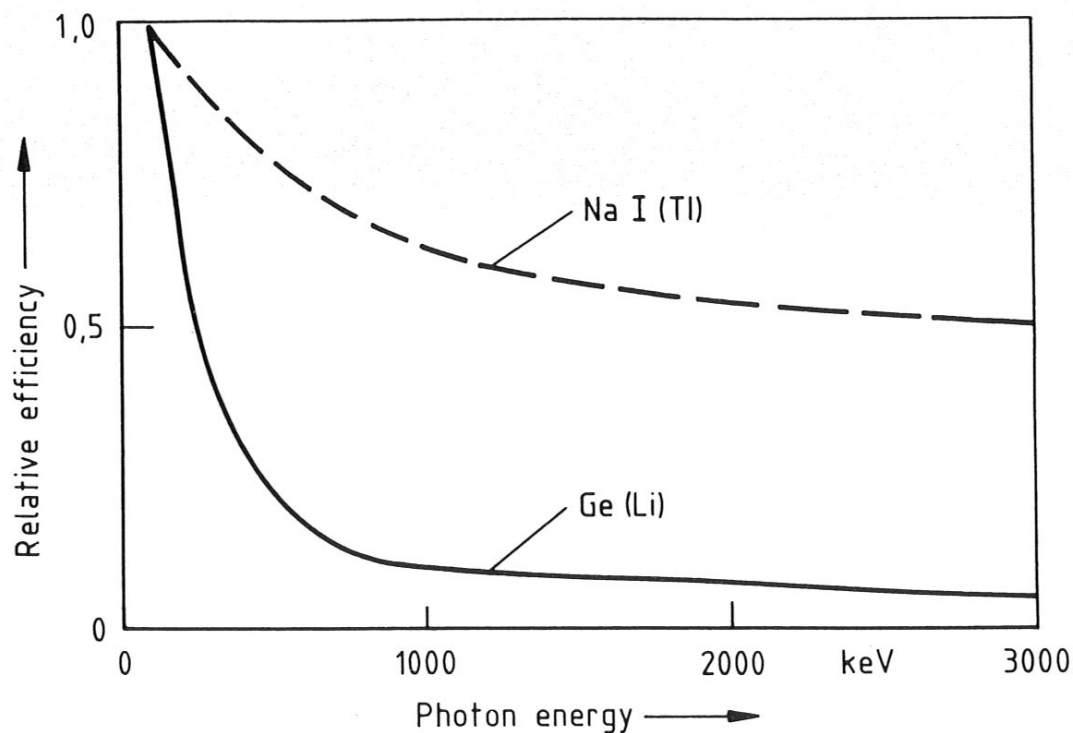


Fig. 4.27: Relative full energy peak efficiency as a function of energy

Slight differences in the curves are due to the different energy absorption functions of both materials (see Fig's. 4.12 and 4.13). The active volume of the crystal is an important parameter which has significant influence upon the photopeak efficiency; in large crystal volumes photon-ray energies are more likely to be absorbed entirely than in small ones. Scintillation crystals are favoured with respect to active volumes since, until nowadays, semiconductor crystal active volumes are restricted for different reasons (Büker⁴¹⁶), whereas, for instance, NaI scintillation crystals can be produced in very large volumes and practically any geometrical shape⁵¹⁷. However, with advancing solid state technology, the availability of semiconductor crystals with active volumes comparable to those of standard NaI crystals may be expected in the near future. This does not necessarily result in the same photopeak counting efficiency, of course, because of other parameters which are mentioned above and will be named in the following, but Ge(Li)-detectors with counting efficiencies up to 40% of that of a standard NaI crystal counter (see 4.4) are not unusual nowadays. See also⁴⁸⁷.

Both the crystal density and its average atomic number are determining factors for the counting efficiency of a detector, since they determine the rate of absorption of the incident photons. The density of germanium is higher than that of NaI (see table 4-1), but, in terms of average atomic number, NaI is superior.

It is clearly shown that scintillation detectors, particularly NaI crystals, are superior to semiconductor detectors with respect to photopeak counting efficiency. Therefore, if photon spectra have to be measured which contain only one or a few energy lines which are not located too closely in their energies, the analyst will surely select a NaI detector for its greater efficiency's sake, and, as will be shown in the following, not only for it. This is especially the case if after activation a radiochemical separation is carried out followed by subsequent measurement of the single components. There is no point in using a high-resolution detector - abandoning the mentioned higher efficiency of an NaI crystal - if no spectral interference by neighbouring gamma energies have to be taken into account. A typical example is the photon activation analysis of light elements which have to be separated from the matrix after bremsstrahlung exposure. This is discussed further in chapter 6.1.

The efficiency behaviour of low energy photon planar semiconductor diodes is essentially different in the energy region for which they are designed (see Fig's. 4.6 and 4.7). In the very low energy part their counting efficiency is

primarily dependent upon the radiation absorption in the beryllium front window and in the inactive surface partition of the crystal. The efficiency curve, with increasing photon energy, then increases rapidly to 100% absorption of the incident radiation. The efficiency function of a germanium low energy photon diode shows a pronounced K-absorption edge and then, from about 60 to 80 keV upwards (this depends upon the active thickness of the crystal) decreases. The efficiency function of a Si(Li)-detector shows essentially the same shape, except for the fact that the Si-edge is not visible since it is not very high and the detector efficiency in these low energy regions is poor. Due to the low atomic number of the material, the descent of the efficiency curve starts at lower radiation energies than is the case in germanium detectors.

More information about the intrinsic sensitivity of detectors, germanium and silicon diodes in particular, can be found in Ref's. 487-492.

4.1.4.4 Signal-to-Compton ratio

As outlined in paragraph 4.1.3, the Compton continuum is an unavoidable source of interference. The major partition of the total background of a pulse height spectrum is due to the Compton effect. Therefore, one strives for the largest possible photopeak-to-Compton ratio. It is primarily dependent upon the detector size and material and the incident photon energy as indicated in Fig's. 4.12-4.18. If one compares both detector systems with respect to signal-to-Compton ratio, one has to differentiate between two points of view: first, the ratio between the integrals of the photopeak and the Compton continuum, and second the ratio between the height of both. In the first case, the NaI crystal is superior due to its higher average atomic number having a greater photopeak efficiency.

It is evident that the active volume of a detector influences the peak-to-Compton ratio. Here again, for technological reasons, the NaI crystal is superior since the active volumes of semiconductor detector crystals, as outlined in the preceding paragraph, are rather limited as yet. However, in the photon spectroscopy practice, the height ratio between the photopeak and the Compton continuum is much more relevant than that of their integrals since the analytical quality of a photopeak is determined - among other criteria - by its height compared to the background height directly beneath it. Therefore, the energy resolution of the detector influences strongly a peak-to-Compton height ratio because, along with improving energy resolution, peaks get narrow and relatively high whereas the height of the Compton continuum does not change signifi-

cantly with increasing energy resolution capability. The peak-to-Compton ratio of a high-resolution spectrometry system is also indirectly dependent upon the count rate because of the degradation of the energy resolution with increasing count rates to be measured (see above, 4.1.4.1). In the case of low energy photon spectroscopy with planar semiconductor diodes one usually does not have to take into account significant Compton background since at low energies photons most likely transfer their energies to the detector by photoeffect interaction, so that the photopeaks in a low energy photon spectrum generally are superimposed upon a reasonably low background (Fig.4.25).

4.1.4.5 Relationship between photon energy and pulse height

The pulse heights obtained by most of the energy-discriminating radiation detectors are proportional to the energy of the incident photons. This statement is valid under two conditions. First, total energy transfer to the active part of the detector is assumed, that means that the photopeak only is considered. Second, the measured photopeaks are located within the linearity of the spectrometer.

In activation analysis, application of scintillation and semiconductor detectors both conditions are fulfilled since first, generally only photopeaks are considered during spectrum analysis (according to the knowledge of the authors there is but one exception, namely the inclusion of the escape lines of ^{16}N into the quantitative spectrum evaluation in the case of oxygen analysis by (n,p)-reaction with a neutron generator¹¹). Second, the photon energies of interest in activation analysis are located within the linear partition of the spectrometer in any case.

There have been attempts to fit a higher order function to the energy calibration points (see paragr. 4.4) but it has turned out that this procedure is of doubtful value and the achievable gain of energy determination accuracy is not significant for activation analysis application⁵¹⁴.

4.1.4.6 Energy limits of the measurable photon spectrum

In the preceding paragraph it was mentioned that all energies of interest for the activation analyst lie in the linear energy range of the detectors. Thus, these limits are determined by several influence parameters other than the linearity range of the spectrometer. Theoretically, there is no upper energy measuring limit, but as obvious in Fig.4.27, at very high energies the photo-

peak efficiencies rapidly decrease so that the achievable analytical sensitivity is poor. On the other hand, there are two good reasons for the analytical application of high photon energies, namely the favourable signal-to-background ratio at high energies, and the fact that spectral interference is less probable (see chapter 5). Nevertheless, normally one does not use gamma-ray lines exceeding say 3.5 MeV.

Physically, like in the case of high energies, there is no lower limit of measurable energies in both detector systems under consideration. Practically, the lower limit is determined primarily by the photon absorption in the detector housing and, if present, the radiation entrance window. As mentioned above, planar low energy photon semiconductor diodes and also flat configured NaI crystals usually are equipped with thin windows of a low atom number material, typically beryllium, to allow the entrance of soft radiation into the detector crystal. The lower limit of the measurable energy spectrum is also visible in the efficiency curve representations (Fig's. 4.6 and 4.7). There is no significant difference concerning the measurable energy range between large volume NaI crystals on one hand and large coaxial semiconductor detectors on the other hand; usually both are applied for measurement of photon energies from about 90 keV upwards.

4.1.4.7 Detector geometries available

In this paragraph two geometrical detector features are discussed, namely the cryostat configuration used in semiconductor detectors and the shape of the detector crystal.

The cryostats of semiconductor detectors are manufactured in a large variety of geometries (see Fig. 4.9) which do not have any influence upon the counting properties of the crystal but are rather provided for the user's convenience in installing special apparatus setups; semiconductor detectors, due to their liquid nitrogen supply vessel, require a lot of storage room (see next paragraph), and the analyst sometimes might have to optimise the total spectrometer setup geometry in accordance to the space available in the laboratory. Instead, NaI detectors are comparatively small-sized in general, and therefore usually there is no difficulty concerning laboratory space. The shape of the crystal in both kinds of detector has significant influence upon all aspects of the counting behaviour. As shown in paragraph 4.1.1 NaI-crystals can be supplied in almost any geometry, whereas semiconductor detectors are somewhat limited with respect to both crystal shape and active volume. This is due to the more com-

plicated way of creating the active zone in the crystal. In Fig.4.2 standard NaI-crystal geometries available are represented, and in Fig.4.4 the semiconductor detector configurations usually supplied by the manufacturers are shown. For activation analysis, however, simple plain or well-type NaI crystals and large volume coaxial semiconductor detectors or planar low energy photon diodes are used almost exclusively. As noted in chapter 4.1.1, the use of well-type germanium detectors for quasi- 4π -counting would entail a gain in counting efficiency but also enhance the complexity of the resulting spectra, especially in the case of multi-component samples to be counted which emit a large number of photon energies⁴⁹³. These detectors usually are applied for the measurement of extremely low activities, e.g. in the low-level counting of radioactive pollutants in the environment.

4.1.4.8 Miscellaneous aspects and summary

In this paragraph, NaI- and Ge-detectors are compared regarding parameters which cannot exactly be quantified. A table is presented which gives a summary of all above discussed parameters comparatively for both detector systems considered. As already touched on, one of the most significant differences is the necessity of the cooling by liquid nitrogen of germanium detectors (at least during application of the operating bias voltage), whereas NaI crystals have a wide operating temperature range which includes room temperature. The cooling of the germanium crystals entails considerable complication in the handling of the detectors. First, due to the Dewar vessel for the liquid nitrogen supply, relatively large storage room is required for the detector. Second, especially in the case of drifted germanium detectors the cooling has to be provided absolutely continuously; interruption of the cooling would cause severe damage of the crystal and parts of the electronic equipment. Therefore, the proper operation of the cryostat system of a semiconductor detector has to be observed continuously to provide, in the case of irregular functioning, immediate repair to avoid fatal warm-up of the crystal. Thus germanium detectors require considerable maintenance effort whereas NaI detectors are comparatively easy-to-handle. This also includes the transportability of the spectrometers.

There are also differences in the mechanical stability of both detector systems, but this is not relevant in the case of activation analysis application since, once installed, the detectors generally are not exposed to mechanical shocks.

The total durability i.e. the life period of the detectors intrinsically are